

the usual estimate of the anomalous diffusion associated with the presence of electrostatic fluctuations. The diffusion coefficient is⁸

$$D \simeq \sum_k \frac{\gamma_k}{\omega_k^2} \left(\frac{k_\theta \varphi_k c}{B} \right)^2,$$

where φ_k is the amplitude of the electrostatic potential of the \vec{k} mode, ω_k and γ_k are the real and the imaginary part of the frequency, k_θ is the poloidal component of the wave vector, and the sum is over all the existing modes. For a low-frequency electrostatic wave we can take $\tilde{n}_k/\tilde{n}_e \simeq e\varphi_k/T_e$. If $\gamma_k/\omega_k \simeq 10^{-1}$ the level of the observed fluctuations accounts for the total electron losses of the ATC discharge.⁴

In conclusion I have observed a new class of small-scale density fluctuations in the ATC tokamak. Their frequency spectrum is consistent with that of drift waves and their amplitudes are maximum in the range of wavelengths where the transverse inertia of ions plays a role in the plasma stability. The amplitude of these fluctuations are sufficient to explain a large fraction of the electron energy losses of ATC.

I am grateful to H. P. Furth and R. A. Ellis for

their encouragement and support and to F. W. Perkins and T. H. Stix for useful discussions. I should also like to express my particular appreciation to R. Shoemaker and his crew of technicians for their help in the operation of the ATC device.

*Work supported by the U.S. Energy Research and Development Administration Contract No. E(11-1)-3073.

¹B. B. Kadomtsev and O. P. Pogutse, Nucl. Fusion **11**, 67 (1971).

²S. O. Dean *et al.*, U.S. Atomic Energy Commission Report No. WASH-1295, 1974 (unpublished).

³M. N. Rosenbluth and N. Rostoker, Phys. Fluids **5**, 776 (1962).

⁴K. Bol *et al.*, Phys. Rev. Lett. **29**, 1495 (1972).

⁵C. S. Liu, M. N. Rosenbluth, and C. W. Horton, Phys. Rev. Lett. **29**, 1489 (1972).

⁶B. Coppi, Phys. Rev. Lett. **25**, 851 (1970); N. T. Gladd and C. W. Horton, Phys. Fluids **16**, 879 (1973).

⁷B. B. Kadomtsev and O. P. Pogutse, Dokl. Akad. Nauk SSSR **186**, 553 (1969) [Sov. Phys. Dokl. **14**, 470 (1969)].

⁸B. Coppi and E. Mazzucato, Phys. Fluids **14**, 134 (1971), and references therein.

Shock Waves Generated by an Oscillating Electric Field in an Expanding Plasma

H. Ikezi

Bell Laboratories, Murray Hill, New Jersey 07974

and

K. Mima and Kyoji Nishikawa

Faculty of Science, Hiroshima University, Hiroshima, Japan

and

Masaaki Inutake

Institute of Plasma Physics, Nagoya University, Nagoya, Japan

(Received 17 July 1975)

A strong radio-frequency field applied to an expanding plasma is found to produce a shock at the surface where the local plasma frequency matches the applied frequency. The shock propagates towards the upstream overdense region with the ion-acoustic speed relative to the plasma flow. The density jump at the shock front is found to be proportional to the field amplitude.

Recent experiments^{1,2} and numerical simulations³ have indicated that when an intense oscillating electric field is applied to a plasma, it modifies the plasma density profile and makes plasma cavities near the plasma wave cutoff where the applied pump field frequency ω_0 equals the local

electron plasma frequency ω_{pe} . In contrast to the above experiments which have been carried out in a stationary plasma, a laser-produced plasma interacts with the laser light while the plasma is expanding. In the present experiment, we intend to study the evolution of the plasma density in an

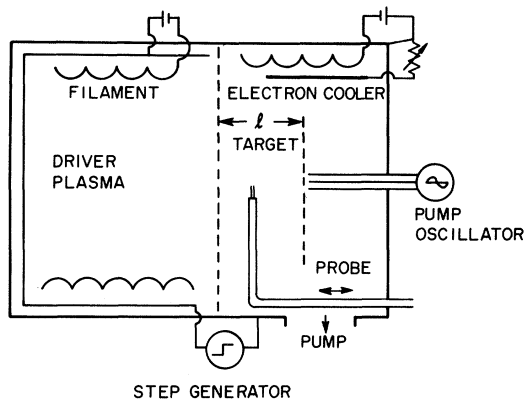


FIG. 1. Experimental setup.

expanding plasma due to interaction with a radio-frequency field. We have experimentally found that a shock wave is formed in contrast to the previous experiments where cavities (or solitary waves) were observed. This observation verifies the recent computer simulation results.⁴

The experiment was carried out in a double plasma device⁵ illustrated in Fig. 1. Two argon plasmas are produced independently on both sides of a mesh grid located at the middle of the vacuum chamber (40 cm in diameter and 70 cm in length). An additional grid (20 cm in diameter) which is set in the target plasma (on the right-hand side) applies high-frequency electric field at a few hundreded megahertz to the plasma between two grids. The separation, l , of the grids is 14 cm. The plasma parameters are the ion temperature $T_i \approx 0.2$ eV and the argon gas pressure $p = (1-3) \times 10^{-4}$ Torr. The electron temperature T_e is continuously controllable in range from 0.5 to 4 eV by regulating the discharge currents to the semiconductor-coated chamber wall and the metallic electrode (the electron cooler, see Fig. 1).

A potential step applied to the driver plasma on the left-hand side injects the ions into the target plasma. The electrons produced in the target plasma neutralize these additional ions. The streaming velocity of injected ions is controllable. When $T_e > 1.5$ eV, the injected ions produce electrostatic shock waves⁶ by interacting with the background plasma without the pump field. For $T_e \lesssim 1.5$ eV, the electrons shield injected ions, and no shock discontinuity appears in the density profile. In Fig. 2, the spatial density distributions (upper diagram) and the ion distribution plotted in the energy-distance plane are shown at 10- μ sec intervals after the start of ion

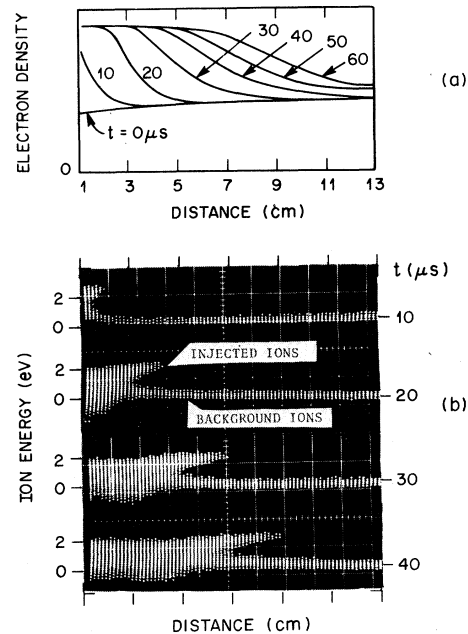


FIG. 2. (a) Spatial electron density profile and (b) ion distribution plotted in the energy-distance plane at indicated times after ion injection. No rf field is applied.

injection into the target plasma. These diagrams indicate that the plasma expands smoothly without generating any ion-ion two-stream instability.⁷⁻⁹ This feature of the plasma expansion is described by a "self-similar" solution of the fluid equations for ions shielded by isothermal electrons.^{10,11}

We now look at the effects induced by the high-frequency pump field imposed on the plasma parallel to the density gradient. The density profiles with and without the pump field are plotted in Figs. 3(a) and 3(b). The background plasma frequency is well below the pump frequency. After the ions are injected, the high-frequency field makes a sharp density jump with a width of 4 mm (≈ 20 Debye lengths, λ_D) at the middle of the slope, where the local electron plasma frequency equals the pump frequency ($\omega_p/2\pi = 330$ MHz). The non-uniformity scale length, $L \equiv n/(\partial n/\partial x)$, of the unperturbed plasma at this initial time is $(2-3) \times 10^2 \lambda_D$. A train of oscillations with the wavelength of $40 \lambda_D$ appears on the plateau formed on the downstream side [the right-hand side in Fig. 3(b)] of the shock jump. The parametric decay instability,^{12,13} generating an ion-acoustic wave ($\omega_s/2\pi \approx 0.2$ MHz $\approx 0.2 \omega_{pi}/2\pi$) and a lower sideband to the pump in the plateau region, also starts growing at 50 μ sec after the ion injection. (The data-sampling processing employed in plot-

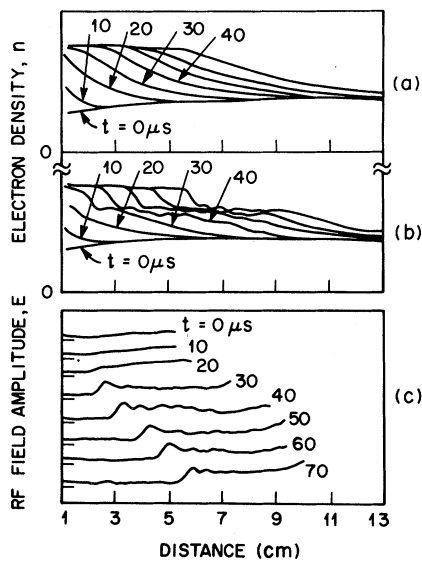


FIG. 3. Electron density profile: (a) without rf field; (b) with rf field. (c) Spatial rf field amplitude distributions, showing enhancement of the field amplitude at shock front.

ting Fig. 3 averages out the decay instability signals.) However, this instability saturates at a very low level compared to the shock jump; the instability density fluctuation is 1–2% of background density. An enhancement of the high-frequency electric field is found on the downstream side of the shock. The enhancement of the amplitude is observed to reach a value 5 times as large as the amplitude before the shock sets in (see Fig. 4). The profile of the high-frequency field intensity also reveals spatial oscillations which correspond to the one appearing in the density distribution.

The amplitude of high-frequency field is measured by detecting the potential difference between two wire probes. The probe size is chosen in such a way that the scale length of the plasma-probe interaction region is comparable to the Debye length, so that the transit-time damping³ (or the Landau damping)¹⁴ suppresses¹⁵ the resonant decoupling of the probe from the plasma, which may occur at the plasma frequency. In order to check the effect of the high-frequency field on the probe measurements, the pump power is turned off at a time we desire to measure the density profile. The spatial distributions of the electron saturation current to the plane probe right before and after the turning off of the pump do not show any significant difference.

The propagation velocity of the shock is slower

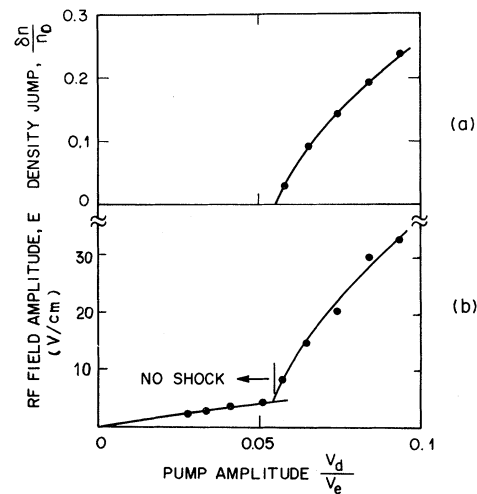


FIG. 4. (a) Density jump and (b) rf field amplitude at the shock front as a function of pump field amplitude v_d/v_e .

than the streaming-ion velocity. We launch ion-acoustic pulses on the slope of the expanding plasma by applying a pulse signal to the grid separating the two plasmas. A single excitation pulse generates both the fast and the slow waves on the streaming ions.^{9, 16} From this experiment, we have found that the velocity of the slow wave is approximately equal to the shock velocity, indicating that the present shock wave propagates against the ion stream with the ion-acoustic velocity. Since the ion-acoustic velocity is smaller than the ion-streaming velocity, the shock moves in the laboratory frame in the ion-stream direction. We note here that the ion-acoustic velocity in the streaming-ion frame is smaller than $(T_e/M)^{1/2}$ because of the presence of background ions.⁹ We have carried out experiments with a pump frequency ranging from 200 to 400 MHz and have found that all above features do not depend on the pump frequency, provided the plasma density is adjusted in the way described before. The extent of the shock in the direction perpendicular to its propagation direction is approximately the same as the diameter of the grid.

The shock wave occurs when the pump intensity is above a threshold value. Both the amount of density jump δn and the oscillating electric field amplitude E measured at the shock front are plotted in Fig. 4 as a function of pump amplitude v_d/v_e . (When no shock takes place, E is measured at the cutoff surface.) Here, v_e is the electron thermal velocity $(T_e/m)^{1/2}$, and v_d the oscillating electron velocity defined by $v_d = eE_0/m\omega_0$, where E_0 is the electric field defined by $E_0 = \phi_0/$

l , with ϕ_0 the rf voltage applied between the grids. The shock is generated when $v_d/v_e > 0.055$. We also find a linear relationship between δn and E above the threshold. In a nonuniform plasma, however, the pump field is not spatially uniform; it is enhanced at the cutoff surface.^{17,18} Therefore, the actual threshold is higher than the above value.

We interpret the above experimental results as follows. After the ions are injected, the enhanced local plasma frequency matches the pump frequency. Then the pump field induces the modulational instability¹⁹ (the oscillating two-stream instability) at the cutoff surface. Although the instability generates a localized density depression, this depression cannot trap the electron plasma wave, because the density gradient due to the plasma expansion at this time is as large as the density gradient due to the instability. Since the electron plasma wave excited at the cutoff surface propagates out to the underdense region, and its amplitude becomes uniform, the ponderomotive force²⁰ maintains only the shock front where the turning point of the electron plasma wave is located. The plasma expansion makes the density uniform on both sides of the shock jump; the plasma-oscillating-field system thus approaches a stationary shock state. As a possible explanation of this shock wave, we have found analytically a stationary shock solution in a plasma-oscillating-field system by taking into account a deformation of the electron distribution function due to reflected electrons in the upstream overdense region.²¹ The theory is based on the fact that the shock moves in resonance with the acoustic motion. The resonance yields a linear relationship between the density perturbation and the field amplitude²² as observed in the present experiment.

The authors acknowledge the help of Dr. D. Forslund who pointed out the need for experi-

ments in an expanding plasma.

¹H. Ikezi, K. Nishikawa, and K. Mima, J. Phys. Soc. Jpn. **37**, 766 (1974).

²H. C. Kim, R. Stenzel, and A. Y. Wong, Phys. Rev. Lett. **33**, 886 (1974); A. Y. Wong and R. Stenzel, Phys. Rev. Lett. **34**, 206 (1975).

³E. J. Valeo and W. L. Kruer, Phys. Rev. Lett. **33**, 750 (1974).

⁴D. W. Forslund, J. M. Kindel, K. Lee, and E. L. Lindeman, Phys. Rev. Lett. **36**, 35 (1976).

⁵R. J. Taylor, K. R. MacKenzie, and H. Ikezi, Rev. Sci. Instrum. **43**, 1675 (1972).

⁶H. Ikezi, T. Kamimura, M. Kako, and K. E. Lonngren, Phys. Fluids **16**, 2167 (1973).

⁷T. E. Stringer, Plasma Phys. **6**, 267 (1964); B. D. Fried and A. Y. Wong, Phys. Fluids **9**, 1084 (1966).

⁸R. J. Taylor and F. V. Coroniti, Phys. Rev. Lett. **29**, 34 (1972).

⁹Y. Kiwamoto, J. Phys. Soc. Jpn. **37**, 466 (1974).

¹⁰I. Alexeff, K. Estabrook, and M. Widner, Phys. Fluids **14**, 2355 (1971).

¹¹R. J. Mason, Phys. Fluids **15**, 845 (1972).

¹²R. A. Stern and N. Tzoar, Phys. Rev. Lett. **17**, 903 (1966).

¹³R. Stenzel and A. Y. Wong, Phys. Rev. Lett. **28**, 274 (1972).

¹⁴E. A. Jackson and M. Raether, Phys. Fluids **9**, 1257 (1966).

¹⁵J. A. Waletzko and G. Bekefi, Radio Sci. **2**, 489 (1967).

¹⁶N. Sato, H. Sugai, and R. Hatakeyama, Phys. Rev. Lett. **34**, 931 (1975).

¹⁷R. Stenzel, A. Y. Wong, and H. C. Kim, Phys. Rev. Lett. **32**, 6541 (1974).

¹⁸G. J. Morales and Y. C. Lee, Phys. Rev. Lett. **33**, 1016 (1974).

¹⁹K. Nishikawa, J. Phys. Soc. Jpn. **24**, 916, 1152 (1968).

²⁰L. D. Landau and E. M. Lifshitz, *Electrodynamics of Continuous Media* (Pergamon, New York, 1960), Eq. (15.14).

²¹K. Mima, K. Nishikawa, and H. Ikezi, Phys. Rev. Lett. **35**, 726 (1975).

²²K. Nishikawa, H. Hojo, K. Mima, and H. Ikezi, Phys. Rev. Lett. **33**, 148 (1974).

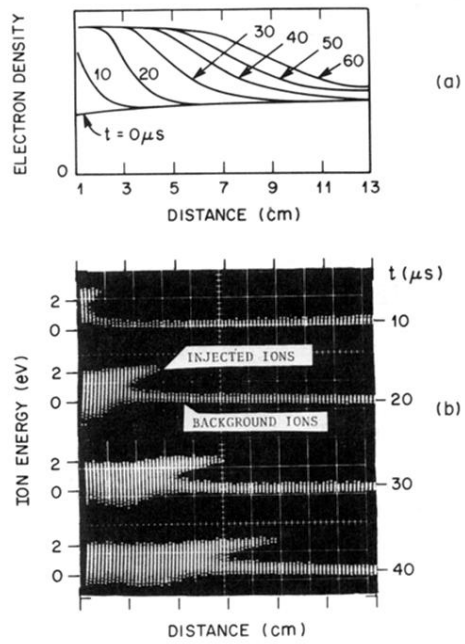


FIG. 2. (a) Spatial electron density profile and (b) ion distribution plotted in the energy-distance plane at indicated times after ion injection. No rf field is applied.